Multi-Carrier CDMA in Rayleigh Fading Channel

Jean-Paul Linnartz and Nathan Yee

[1]Dept. of Electrical Engineering and Computer Science
University of California, Berkeley 94720
Telephone: 510-643-8351 E-mail: linnartz@eecs.berkeley.edu

Abstract: The application of Wiener filtering to the detection of Multi-Carrier Code Division Multiple Access (MC-CDMA) signals is analyzed. An analytical model is developed to evaluate an MC-CDMA system with a very large number of subcarriers. This model is compared with simulations for 8 and 64 subcarriers. Simulation results are also presented on the effect of correlated fading (in the frequency domain) at the subcarriers .

I. Introduction

In an earlier paper, the authors discussed the utilization of MC-CDMA as a digital modulation and multiple access technique in an indoor wireless environment [1]. Due to its special signal structure, MC-CDMA signals will not experience significant linear distortion in fading channels where the symbol duration, T_b, is much larger than the delay spread, T_d.

With orthogonal MC-CDMA [2], each data symbol is simultaneously transmitted at N binary phase shift-keying (BPSK) narrowband subcarriers, each separated by F/T_b Hz where F is an integer. As shown in the transmitter model of Fig. 1, each of the N subcarrier waveforms is modulated (multiplied) by a single (time constant) chip belonging to a spreading code of length N. Different users transmit at the same set of subcarriers but with a different spreading code in the frequency domain. In contrast to Direct-Sequence CDMA [3] (or other wideband) signals, MC-CDMA signals are not significantly affected by delay spreads due to their narrowband composition. This modulation technique should not be confused with transmitting multiple DS-CDMA signals at different frequencies as done so in [4]. Note that the signal structure of MC-CDMA is similar to that of Orthogonal Frequency Division Multiplexing (OFDM) [5] but the manner in which the signals are used is very different .

While the general shape of each individual subcarrier will not experience significant linear distortion after transmission, the flat fading that each subcarrier with experience results in an amplitude scaling. Unequal scaling a different subcarriers distorts the orthogonality between users. While the conventional detection methods of equal gain combining (EGC) and maximal ratio combining (MRC) may be sufficient in an additive white Gaussian noise (AWGN) channel, these detection

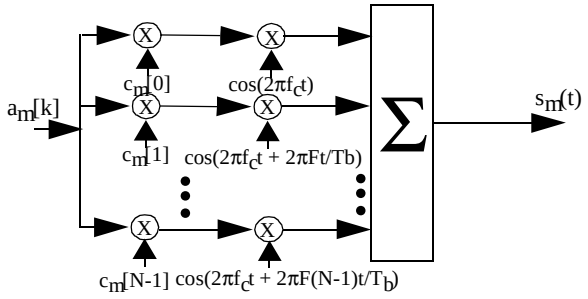

Fig. 1 Transmitter Model of the *mth* user

methods do not directly address the issues of orthogonality and of interference cancellation. Consequently, these detection methods do not perform as well in interference limited channels.

In this paper, we will apply Wiener filtering to the detection of MC-CDMA signals. Wiener filtering is optimal in a mean-squared error sense with respect to both the noise and the interference. In most fading channels, the determination of the Wiener coefficients is performed adaptively. In this paper, we are primarily concerned with the theoretical limits and not the implementation aspects of how to track the channel fluctuations [6]. Thus, it is assumed that accurate estimates of the complete channel state information (i.e., the fading at the subcarriers) are available and that the Wiener coefficients are chosen accordingly.

II. Channel Model

Denote the vector of the data symbols by

$$A = \left[a_0[k] \;\; a_1[k] \;\; \ldots \;\; a_{N-1}[k]\right]^T \tag{1}$$

where $a_m[k] \in \{-1, 1\}$ corresponds to the data symbol of the *mth* user. If user m is inactive, then $a_m[k] = 0$. Define the code matrix C to be

$$C = \begin{bmatrix} c_0[0] & c_1[0] & \ldots & c_{N-1}[0] \\ c_0[1] & c_1[1] & \ldots & c_{N-1}[1] \\ \ldots & \ldots & \ldots & \ldots \\ c_0[N-1] & c_1[N-1] & \ldots & c_{N-1}[N-1] \end{bmatrix} \tag{2}$$

where the *mth* column vector of C corresponds to the spreading code, $\{c_m[i] \mid i = 0, 1, \ldots, N-1\}$, of the *mth* user. Using the vector and matrix notation described above, an equivalent discrete vector representation of the transmitted signal described in Fig. 1 is

$$S = \left[s_0[k] \;\; s_1[k] \;\; \ldots \;\; s_{N-1}[k]\right]^T = CA \tag{3}$$

where $s_i[k]$ represents the signal components of all users at the *ith* subcarrier for the *kth* symbol interval. The actual continuous-time transmitted signal corresponding the *kth* data symbol of the *mth* user, $a_m[k]$, is

$$\begin{aligned} s_m(t) &= a_m[k] \sum_{i=0} c_m[i] \cos\left\{2\pi\left(f_c + \frac{F}{T_b} i\right)t\right\} \\ &\quad \times p_{T_b}(t - kT_b) \end{aligned} \tag{4}$$

where f_c is the carrier frequency and $p_T(t)$ is a unit pulse that is non-zero for $t \in [0, T)$ and zero otherwise. Note that in a distortionless channel, that data symbol of the *mth* user can be recovered using the orthogonality of the codes as indicated by the following operation

$$a_m[k] = \frac{1}{N} C_m \bullet S \tag{5}$$

where $\bullet$ denotes the inner product between two vectors and

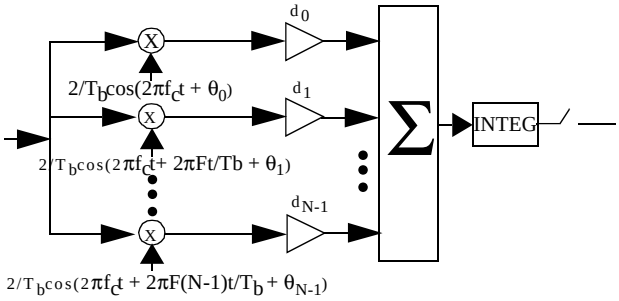

Fig. 2 Receiver Model

$$C_m = \left[c_m[0] \;\; c_m[1] \;\; \ldots \;\; c_m[N-1]\right]^T \tag{6}$$

is a vector containing the spreading code of the *mth* user.

In this paper, we will focus on downlink transmissions, i.e., from the base station to the mobiles. Assuming that the delay spread is much smaller than the symbol duration, the effect of the channel at the *ith* subcarrier may be approximated by a constant amplitude scaling, $p_i[k]$, and a constant phase offset, $\theta_i[k]$, over the symbol duration. Using this assumption, the index k will be suppressed throughout the rest of this paper. Applying the received signal to the receiver model shown in Fig. 2, the equivalent discrete representation of the received signal is

$$Y = \left[y_0 \; y_1 \; \ldots \; y_{N-1}\right]^T = HCA + N_1 \tag{7}$$

where y_i represents the component of the received signal at the *ith* subcarrier, the channel matrix H is defined to be

$$H = \begin{bmatrix} \rho_0 & \ldots & 0 & 0 \\ \ldots & \rho_1 & \ldots & 0 \\ 0 & \ldots & \ldots & \ldots \\ 0 & 0 & \ldots & \rho_{N-1} \end{bmatrix}, \tag{8}$$

and $N_1 = \left[\eta_0 \; \eta_1 \; \ldots \; \eta_{N-1}\right]^T$ is a vector containing the corresponding AWGN terms with η_i representing the noise term at the *ith* subcarrier with power N_0/T_b. Obviously, the discrete representation of the demodulated signal given in Eq.(7) is an approximation. However, under the condition $T_b \gg T_d$, each subcarrier faces a relatively flat channel and Eq.(7) provides a reasonable representation.

The application of Wiener filtering to this received signal involves linearly combining the different subcarrier diversity components to yield the decision variable

$$\nu_0 = D \bullet Y \tag{9}$$

where the vector $D = \left[d_0 \; d_1 \; \ldots \; d_{N-1}\right]^T$ represents the optimal weighting coefficients. These coefficients can also be viewed as an amplitude equalization to compensate for the fading at the subcarriers. Arbitrarily choosing $m = 0$ as the desired signal, the optimal choice of the equalization vector D in the mean-squared sense can be determined to be

$$D = R_{Y|H}^{-1} R_{a_0 Y|H} \tag{10}$$

where

$$R_{Y|H} = E\{YY^T\} = HCE(AA^T)C^TH + \frac{N_0}{T_b}I \quad (11)$$

represents the autocorrelation matrix of the received vector Y and $R_{a_0 Y|H}$ represents the cross-correlation vector between the desired symbol, a_0, and the received signal vector, Y. In the formulation of this method, it is assumed that estimates of the channel amplitudes, $\{\rho_i | i = 0, 1, \ldots, N-1\}$, are available and are consequently treated as deterministic constants.

A closed form solution of Eq.(10) is difficult to obtain except for the case of a full load, i.e., when all N users are active. The corresponding equalization coefficient at the ith subcarrier for a full load is

$$d_i = \frac{\rho_i}{N\rho_i^2 + N_0/T_b} c_0[i] . \quad (12)$$

As expected, Eq.(12) indicates that the linear combination of the subcarrier components should include the inner product of the desired user's spreading code vector with the received signal vector. For small ρ_i, the equalization coefficient should be small to avoid excessive amplification of the noise. For large ρ_i, the correction factor should be proportional to taking the inverse of the channel, $1/\rho_i$, in order to restore the orthogonality between users.

For sufficiently large values of N, the average bit error rate (BER) for the case of a full load may be approximated using Eq.(9) and the Central Limit Theorem by

$$BER \cong \frac{1}{2} erfc \sqrt{\frac{1}{2} \frac{(NEw_i)^2}{N^2\sigma_{w_i}^2 + N\frac{N_0}{T_b}Ev_i^2}} \quad (13)$$

where $w_i = \frac{\rho_i^2}{N\rho_i^2 + N_0/T_b}$ and $v_i = \frac{\rho_i}{N\rho_i^2 + N_0/T_b}$. In obtaining this expression, independent and identically distributed (IID) fading at the subcarriers was assumed.

To study the effect of correlated fading through simulations, the following algorithm for generating correlated Rayleigh r.v.s was used. The correlation between two frequencies separated by $\Delta w = 2\pi F(n-l)/T_b$ radians in a complex gaussian fading channel is given by Jakes [7] to be

$$R_\rho(\Delta w) = \frac{1 + j\frac{2\pi F(n-l)}{T_b} T_d}{1 + \left(\frac{2\pi F(n-l)}{T_b}\right)^2 T_d^2} \frac{2\overline{p_m}}{N} . \quad (14)$$

where $j = \sqrt{-1}$ and $\overline{p_m}$ is the local-mean power of the mth user. Defining $\bar{H}$ as a vector of dimension N whose elements, h_i for $i = 0, 1, ..., N-1$, are the complex correlated gaussian fading variables at the different subcarriers, the autocorrelation matrix of $\bar{H}$, $R_{\bar{H}} = E\bar{H}\bar{H}^*$ (with $\bar{H}^*$ meaning the conjugate transpose of $\bar{H}$), can be determined using Eq.(14). The vector $\bar{H}$ can be generated by taking linear combinations of IID unit normal gaussian r.v.s :

$$\bar{H} = AG \quad (15)$$

where G is a vector of dimension N containing IID unit normal r.v.s. A possible choice of the $N \times N$ transformation matrix A is

$$A = \frac{1}{\sqrt{2}} E\Lambda^{1/2} \quad (16)$$

where E is an $N \times N$ matrix with the eigenvectors of $R_{\bar{H}}$ as its column vectors and $\Lambda \in \Re^{N \times N}$ is a diagonal matrix with the eigenvalues of $R_{\bar{H}}$ as its entries. The relationship between the fading variables of Eq.(8) and $\bar{H}$ is

$$\rho_i = |h_i| . \tag{17}$$

III. Simulation and Numerical Results

Due to the lengthy time consumption of the simulations, results for only spreading factors of $N = 8$ and $N = 64$ were obtained. Shown in Fig. 3 is a plot of the average BER versus the signal-to-noise ratio (SNR) in a Rayleigh fading channel for a full load with $N = 8$. IID fading at the subcarriers is assumed. It is also assumed that all users are received with equal power. Note that the analytical results for Wiener filtering differ significantly from the simulation results for large SNR. This discrepancy is due to the application of the Central Limit Theorem to small spreading factors. Shown in Fig. 4 are the results for $N = 64$. Examining Fig. 3 and 4, it can be seen that Eq.(13) is more accurate for large N. Also included in Fig. 3 are the curves for a single narrowband subcarrier with AWGN, and with and without fading. Note that the performance of MC-CDMA is better than a single narrowband transmission due to frequency diversity even with a fully loaded system.

The average BER versus the SNR for correlated fading was also examined for the case of $N = 8$ (see Fig. 5). The degree of correlation was measured in terms of

$$\alpha = \frac{T_d}{T_b} . \tag{18}$$

Small α's correspond to highly correlated fading at the subcarriers while large α's correspond to IID fading. Ideally, the larger the value of α, the higher the degree of frequency diversity. In a DS-CDMA system, the number of resolvable paths is equal to

$$L = \lfloor N\alpha \rfloor + 1 . \tag{19}$$

Note that for $a = 0.125$ $(L = 2)$ most of the benefits in performance from frequency diversity have already been achieved.

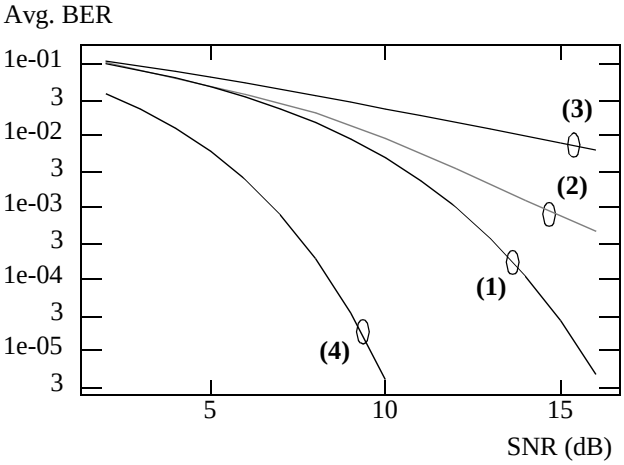

Fig. 3 Average BER vs SNR with Rayleigh fading and a full load for Wiener Filtering: (1) analytical, N -> INF, (2) simulation, N = 8, (3) analytical, N = 1 (single narrowband), and (4) analytical, N = 1 with linear time invariant AWGN channel.

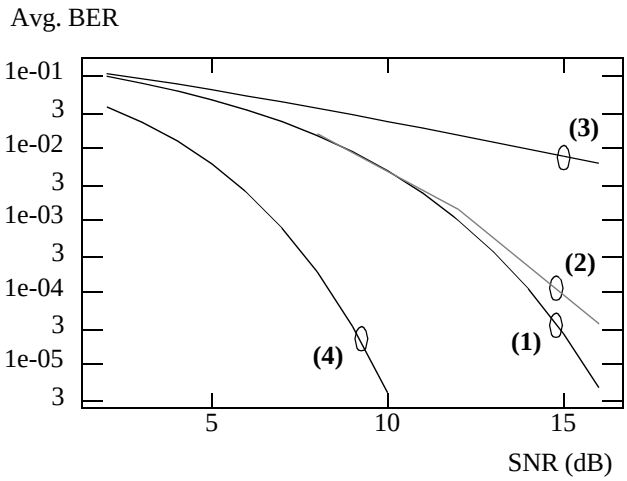

Fig. 4 Average BER vs SNR with Rayleigh fading and a full load for Wiener Filtering: (1) analytical, N -> INF, (2) simulation, N = 64, (3) analytical, N = 1 (single narrowband), and (4) analytical, N = 1 with linear time invariant AWGN channel.

Shown in Fig. 6 is a plot of the simulation results for the average BER versus the number of interferes. The SNR was chosen to be 10dB. Because of the time consuming nature of the simulator, a relatively small spreading factor of $N = 8$ was used. Besides the curves for Wiener filtering, the simulation results of conventional EGC and MRC detection are also included [1]. As expected, Wiener filtering outperforms EGC and MRC substantially in combating interference.

IV. Conclusion

In this paper, the application of Wiener filtering was applied to the detection process of MC-CDMA. In contrast to conventional diversity combining techniques, this detection technique directly addresses the effects of the interference on the BER. It was shown that even with a full load, MC-

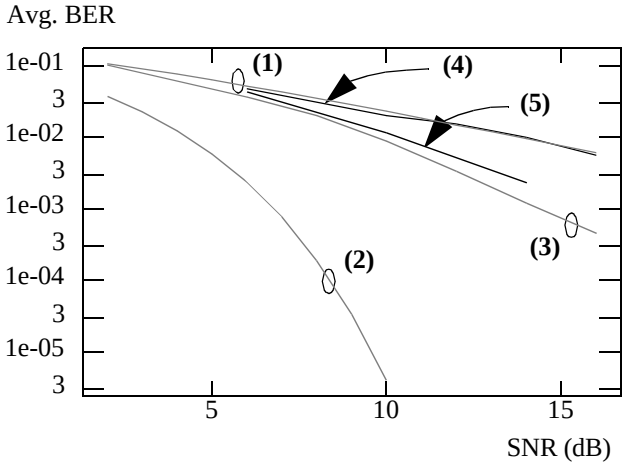

Fig. 5 Average BER vs SNR with Rayleigh fading and a full load for Wiener Filtering: (1) analytical, N = 1, (single subcarrier), (2) analytical, N = 1 with linear time invariant AWGN channel, (3) simulation, N = 8, with IID fading (α = INF), (4) simulation, N = 8, correlated fading with α = 0.001 (L = 1) and (5) α = 0.125 (L = 2).

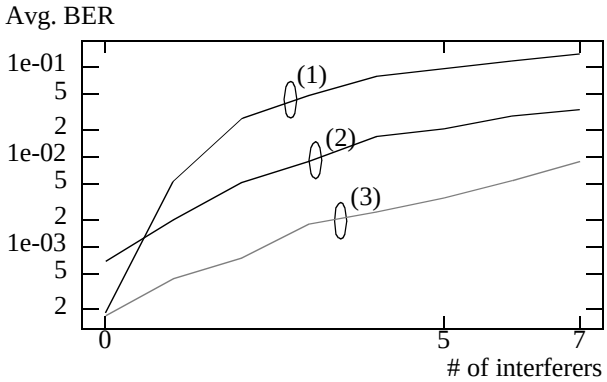

Fig. 6 Average BER vs # of interferers for spreading factor N = 8 with Rayleigh fading and SNR=10dB. Simulation results for (1) Maximal Ratio Combining (2) Equal Gain Combining (3) Wiener filtering.

CDMA with Wiener filtering outperforms single narrowband transmissions in a Rayleigh fading channel. It was also shown that Wiener filtering outperforms conventional detection methods substantially. Analytical approximations for $N \to \infty$ appeared reasonably accurate for SNRs up to 12dB and for $N = 64$ subcarriers. As the number of subcarriers is increased, the accuracy of the analytical results improves.. It was also shown that most of the benefits of frequency diversity can be achieved even in a channel with a significant degree of correlated fading at the subcarriers .

Acknowledgments

Portions of this research have been funded by the California Department of Transportation, Partners in Advanced Transit and Highways (PATH), Teknekron Communication Systems, Berkeley, the University of California MICRO Program and AirTouch International.

V. References

[1] N. Yee, J. P. Linnartz and G. Fettweis, "Multi-Carrier CDMA in Indoor Wireless Radio Networks," *Proceedings PIMRC '93*, Yokohama, Japan, 1993, pp. 109-113.

[2] G. Fettweis, "Multi-Carrier Code Division Multiple Access (MC-CDMA): Basic Idea," Technekron Communication Systems - Internal Report.

[3] R. L. Pickholtz, D. L. Schilling and L.B. Milstein, "Theory of Spread-Spectrum Communications - A Tutorial," *IEEE Transactions on Communications*, COM-30, May 1982, pp. 855-884.

[4] S. Kondo and L. B. Milstein, "MultiCarrier CDMA System with Co-channel Interference Cancellation for an Asynchronous Forward Link", *44th IEEE Veh Tech Conf*, June 7-10 1994, Stockholm.

[5] Leonard J. Cimini, Jr., "Analysis and Simulation of a Digital Mobile Channel Using Orthogonal Frequency Division Multiplexing," *IEEE Transactions on Communications*, vol. COM-33, pp. 665-6.

[6] G. Fettweis, K. Anvari, and A. Shaikh Bahai, "On MultiCarrier Code Division Multiple Access (MC-CDMA) Modem Design", *44th IEEE Veh Tech Conf*, June 7-11 1994, Stockholm.

[7] W. C. Jakes Jr., *Microwave Mobile Communications*, New York: Wiley, 1974.